 CMC, vol.14, no.2, pp.125-140, 2009

Modeling Intergranular Crack Propagation in Polycrystalline Materials

M.A. Arafin[1] **and J.A. Szpunar**[2]

Abstract: A novel microstructure, texture and grain boundary character based model has been proposed to simulate the intergranular crack propagation behavior in textured polycrystalline materials. The model utilizes the Voronoi algorithm and Monte Carlo simulations to construct the microstructure with desired grain shape factor, takes the texture description of the materials to assign the orientations of the grains, evaluates the grain boundary character based on the misorientation angle - axis calculated from the orientations of the neighboring grains, and takes into account the inclination of grain boundaries with respect to the external stress direction. Markov Chain theory has been applied to ensure the crack-path continuity and Monte Carlo simulation technique was employed to obtain the various possible orientation distribution of grains for any given texture description and to vary the spatial distributions of different grain orientations in the microstructure. Crack propagation behavior is simulated for both different types of fiber textures commonly found in Molybdenum polycrystals as well as the random polycrystals. The texture intensities and grain shapes were varied, for fiber and random textured samples, respectively, and resulting crack propagation lengths and percolation frequencies were compared.

Keywords: Intergranular Cracking; Texture; Grain Boundary Character; Voronoi Algorithm; Markov Chain, Monte Carlo Simulations.

1 Introduction

Intergranular cracking has always been recognized as one of the major obstacles in producing materials with superior mechanical properties [Lim and Watanabe (1990), Gertsman and Tangri (1997), Watanabe and Tsurekawa (1999)]. It is well-known that the grain boundary character governs such crack propagation process and the solution to this problem lies in applying certain manufacturing techniques

[1] McGill University, Montreal, Canada.
[2] University of Saskatchewan, Saskatoon, Canada

to obtain materials that contain a large fraction of low-energy boundaries which are crack-resistant. However, it is practically not possible to produce materials with grain boundaries that are entirely of low-energy types. In fact, such ideal material is not also required to avoid intergranular fracture because if the low-energy boundary fraction reaches a threshold value, virtually all the cracks can be arrested without having percolation or before the cracks can reach the critical length beyond which fracture is inevitable.

Numerous studies in the literature clearly prove that not all the grain boundaries are alike [see, e.g., Watanabe (1984), Crawford and Was (1992), Lin and Pope (1993, 1995), Pan, Adams, Olson and Panayotou (1996), Tsurekawa, Kokubun and Watanabe (1999), Gertsman and Bruemmer (2001), Arafin and Szpunar (2009a)]. Low angle boundaries (LAB) and low-Σ coincidence site lattice (CSL) boundaries usually have high fracture strengths, while the random high angle boundaries (HAB) are known to be weakest. Even a transgranular crack can become intergranular when the crack-tip meets a HAB due to strong dislocation pile-ups [Shi and Zikri (2009)]. However, there is remarkable dispute on the misorientation angle limit of LAB and the limit of maximum Σ value up to which they can be considered as truly fracture resistant. Although the common trend is to consider 15° as the maximum limit of misorientation angle for the LAB according to the Brandon's criterion, and 29 as the highest Σ value for this purpose, the answer is not really simple and experimental investigations are required to resolve this issue for any given material. Often the fracture strength decreases significantly with the increase of misorientation angle for the LABs and, only very few low-Σ boundaries have the low-energy characteristic. To make the matters worse, sometimes a higher Σ value CSL boundary can be of fracture resistant type compared to its low-Σ value counter-part [Tsurekawa, Tanaka and Youshinaga (1994)]. Therefore, assuming systematically decreasing fracture strength with the increase of Σ value of up to 29 have very little physical meaning unless the experimental values show such behavior.

The most noticeable difficulty, however, is to use realistic microstructure for the crack-propagation studies because, in order to simulate the intergranular crack propagation process, each of the triple junctions (TJs) needs to be considered and the spatial locations of the TJs and the grain boundaries associated with these TJs never show definite symmetry to put them under a common modeling framework. The conventional modeling approach [see, e.g., Wells, Stewart, Herbert, Scott and Williams (1989), Gertsman and Tangri (1997), Palumbo, King, Aust, Erb and Lichtenberger (1991), Jivkov, Stevens and Marrow (2006), Pan, Olson and Adams (1995), Wang, Zou, and Esling (2002)] is to use hexagonal microstructure as the input grain boundary network to avoid the above problem but such microstructure

does not exist in reality and the results obtained from this type of model is rather over-simplified.

Another common problem in modeling the crack-propagation process is to ensure that the crack-path is continuous, that is, a boundary can crack only if the previous boundary is already cracked. Markov Chain theory can overcome this problem [Pan, Olson and Adams (1995), Gertsman and Tangri (1997), Arafin and Szpunar (2009b)] but, again, each triple junction and grain boundary need to be tracked in order to be able to construct Transition Matrix, will be described later, a necessary pre-requisite to carry out the Markovian analysis. In addition, for the same texture description, there are numerous possible orientation distributions of the grains, let alone the spatial distributions of the grain orientations which may also change the crack propagation behavior noticeably. Therefore, Monte Carlo simulations need to be carried out to account for these variables.

In this study, we have overcome the abovementioned difficulties and proposed a novel modeling approach to simulate the crack propagation behavior in polycrystalline materials. Both fiber textured, having a large fraction of low-energy crack-resistant boundaries, and random textured, with predominantly random high angle boundaries, samples were considered. The intensities of the fiber textured samples were changed to obtain various grain boundary character distributions; multiple crack nucleation sites were considered; and microstructures with different grain shape factors were studied.

2 Modeling of Intergranular Cracking in Textured and Random Polycrystals

The model proposed is of integrated nature. It utilizes the Voronoi algorithm (for microstructure construction), Markov Chain theory (to ensure the crack-path continuity), texture and grain boundary misorientation theories (to assign the crystallographic orientation of the grains and calculate the misorientation angle and rotation axis and subsequently determine the character of the grain boundary), and Monte Carlo simulation (to account for the various possible orientations and spatial distribution of the grain orientations for the same texture description). The development of such model is the result of the author's continuous effort, as a part of a large scale project, to construct a realistic microstructure-based intergranular crack propagation model and, therefore, should be viewed as a major advancement with regard to the previously published ones [Arafin and Szpunar (2009b, 2009c, 2009d)]. Details of the Voronoi algorithm, Markov Chain theory and Monte Carlo simulation, along with an example case on how these techniques could be combined together to simulate the intergranular crack propagation process based on a given GBCD, have been described in [Arafin and Szpunar (2009c)]. The new model, however, is more comprehensive in a way that it can take into account the crystallographic descrip-

tions of the grains and evaluates the grain boundary character from the assigned orientations of the neighboring grains. In addition, the individual grain boundary fracture strength, and projected stress on the grain boundary plane are considered while assessing the vulnerability of a grain boundary under a given loading condition.

In the present article, we have used different fiber textures commonly found with Mo as well as the random Mo polycrystals. For the fiber textured samples, the intensity of texture were varied using Gaussian spread defined by half-width. Misorientation angle and axis were calculated based on the orientations of the neighboring grains and, in estimating the misorientation angle, all the 24 crystallography related solutions were considered, that is full solution sets were obtained by premultiplying the rotation matrix with all the 24 symmetry matrices.

The grain boundaries were classified according to the misorientation angle-axis descriptions and the coincident site lattice schemes [Mykura (1980)]. The maximum orientation deviations of the CSL boundaries were taken from the Brandon Criterion (see Eq. 1):

$$\Delta\theta = 15^0\Sigma^{-1/2} \tag{1}$$

The identifications of CSL boundaries were limited up to $\Sigma 29$ type which is a well-established criterion for such purpose because beyond $\Sigma 29$, the boundaries are usually considered to have the same property as those of the random high angle boundaries.

The alignment of grain boundaries with respect to the stress direction is considered while assessing their responses to the applied load. That is, for any given stress, the projection of stress on to the grain boundary plane is calculated and if the resolved stress exceeds the fracture strength of that grain boundary, the boundary is considered to be fractured. Let us illustrate the crack propagation decision strategy with a simple schematic shown in Fig. 1. Assume that the crack-tip is at point 1, the stress is along the y-direction and the crack is moving from left to right. The model will apply the following sequence of checking algorithm to decide whether to crack the boundary (1-8) or, (1-2) or, both or, arrest at the triple junction (point 1).

Step 1: What are the crystallographic orientations of C_1, C_9 and C_2?

Step 2: What are the misorientation angles and axes between grains C_1 and C_9, and $C_1$and C_2?

Step 3: Use Brandon criterion to determine the characters of the boundaries

Step 4: Find the inclination angles of the grain boundary planes with respect to the direction perpendicular to the stress axis

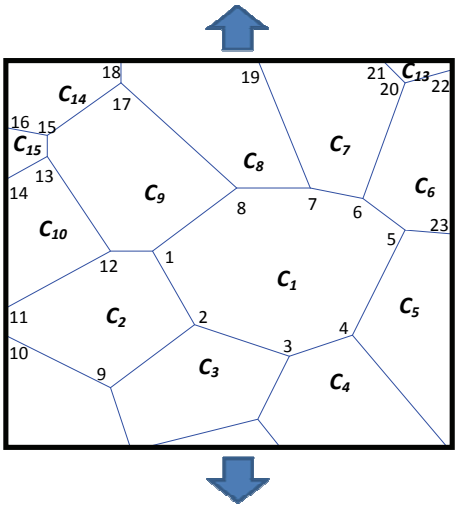

Figure 1: Schematic Voronoi microstructure to illustrate the crack-propagation decision strategy

Step 5: Calculate the projection of stress, σ_p (= σCosθ), on to the grain boundary plane (θ = angle between the grain boundary plane and perpendicular to the stress-axis)

Step 6: If $\sigma_p > \sigma_{GB}$: crack the boundary (σ_{GB}=grain boundary fracture strength)

Steps (1-6) are repeated for all the triple junctions to construct the transition matrix and, subsequently, carry out the Markovian analysis to determine the end-location of the crack(s). Note that, a transition matrix (T_r) is a square matrix (*mxm*) where *m* is the number of triple junctions/nodes in the microstructure. For every triple junction, three T_r elements are obtained based on the above mentioned crack propagation decision algorithm and the remaining elements are assigned to be zero. These elements could be defined either as T_{ii} or T_{ij} type, where, $T_{ii} = 0$ indicates that if the crack-tip arrives at node *i*, it will *not* get arrested here while $T_{ii} = 1$means the opposite, in other words, crack will be arrested at this node. On the other hand, $T_{ij} = 0$ means, if the crack-tip is at node *i*, it will not go to node *j* from there, and $T_{ij} = 1$ indicates the other way around. The initial crack locations are defined with a row vector, $p_{0,}$ and the steady state position of the crack is determined by continue to iterate Eq. 2.

$$p_n = p_0 * T_r^n \tag{2}$$

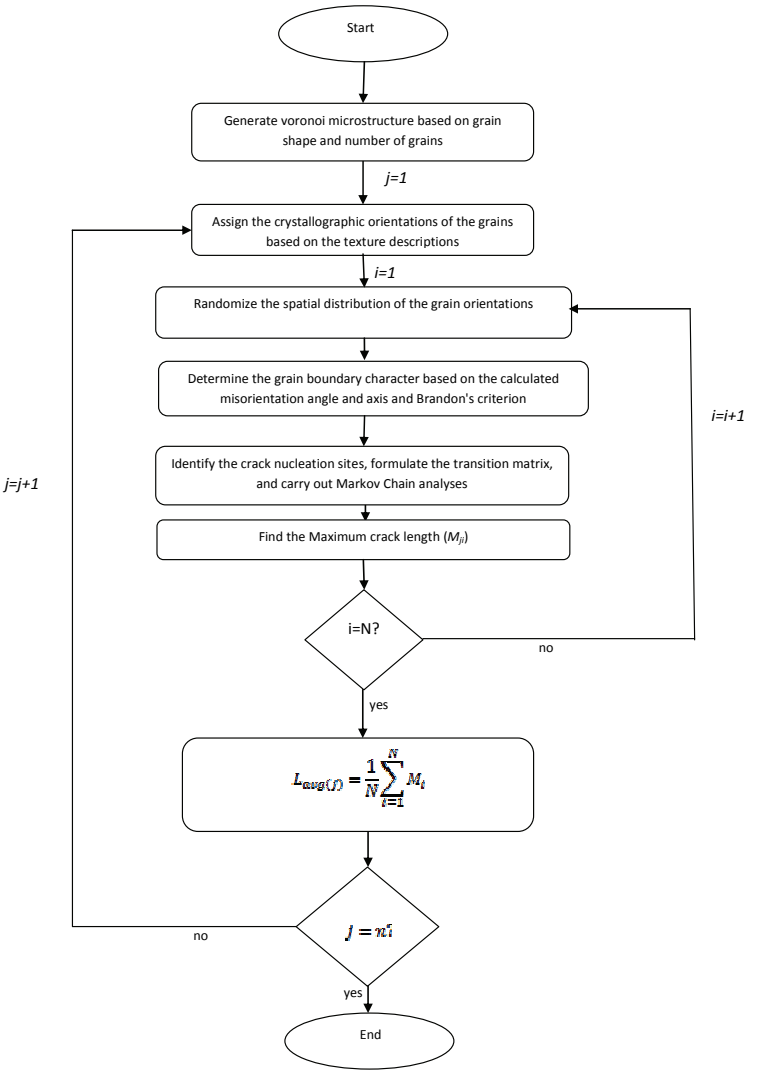

Figure 2: Integrated model algorithm (N= number of Monte Carlo iterations for each microstructure, n = number of different microstructures to be simulated, L_{avg} = normalized average crack-length)

Here, $n = 1, 2, 3, ...s$ and, s is the iteration number for which steady state position is achieved, that is, any further iteration does not lead to the change of crack position.

For each texture description, the spatial distributions of the grain orientations are varied using the Monte Carlo simulation technique. For each simulation, the maximum crack length is recorded and, finally, these lengths are averaged out for the total number of Monte Carlo iterations. The number of times the crack reaches the right hand side of the microstructure is also considered to determine the percolation frequency. The flowchart of the developed integrated model is shown in Fig. 2.

3 Results and Discussions

Key bicrystal experiments were conducted in the literature [Kurishita, Oishi, Kubo, and Yoshinaga (1983), Tanaka, Tsurekawa, Nakashima and Yoshinaga (1994), Ikeda, Morita, Nakashima, and Abe (1999)] to assess the fracture strengths of different types of grain boundaries in Mo at liquid nitrogen temperature to minimize the effect of impurities such as C, O etc. which could significantly alter the desired data. Some studies were also conducted to ascertain the fracture strengths at room temperature [Brosse, Fillit, and Biscondi (1981), Watanabe (1994)] but such data are very limited and do not cover the range of CSL boundaries that are of interests. Therefore, we chose to use this temperature for the model; that is fracture strengths used in the simulations for different types of CSL boundaries, shown in Table 1, are only valid for 77K. The other issue is that although fracture strengths of most of the boundaries within the range of Σ(1-29) are available, CSL boundaries mainly associated with <111> misorientation axis could not be found in the literature. However, these boundaries in Mo were never reported to possess special characteristics and, we assume, in this study, to have the same strength as that of the random boundaries. As pointed out earlier, the fracture strength of Σ1 (LABs) varies considerably within the Brandon limit of 0-15° and, rather than using one single value for Σ1, we used the fracture strengths (also at 77K) based on specific misorientation angle, using data from Kurishita, Oishi, Kubo, and Yoshinaga (1983), Tanaka, Tsurekawa, Nakashima and Yoshinaga (1994), Ikeda, Morita, Nakashima, and Abe (1999), whenever a LAB is identified.

3.1 Model microstructures

In the present study, we have chosen to simulate the crack propagation in a nearly equiaxed microstructure, consists of 1000 grains, as shown in Fig. 3a. However, in order to illustrate the role of grain shape on the resulting crack propagation and percolation frequency, elongated microstructure with low grain shape factor is also considered and discussed in section 3.2. It is worth mentioning here that one of

Table 1: Fracture strengths of different CSL boundaries (up to Σ29) of Mo at 77K

Grain Boundary Type (Σ)	Fracture Strength (MPa)	Reference
3	1750	[Kurisita, Oishi, Kubo, and Yoshinaga (1983)]
5	1193	[Ikeda, Morita, Nakashima, and Abe (1999)]
7	280	-
9	380	[Tanaka, Tsurekawa, Nakashima and Yoshinaga (1994)]
11	480	[Kurisita, Oishi, Kubo, and Yoshinaga (1983)]
13a	975	[Ikeda, Morita, Nakashima, and Abe (1999)]
13b	280	-
15	280	-
17a	865	[Ikeda, Morita, Nakashima, and Abe (1999)]
17b	1450	[Tanaka, Tsurekawa, Nakashima and Yoshinaga (1994)]
19a	280	[Kurisita, Oishi, Kubo, and Yoshinaga (1983)]
19b	280	-
21a	280	-
21b	280	-
23	280	-
25a	1100	[Ikeda, Morita, Nakashima, and Abe (1999)]
25b	280	-
27a	280	-
27b	280	-
29a	1300	[Ikeda, Morita, Nakashima, and Abe (1999)]
29b	280	-

the major advantages of Voronoi algorithm is its ability to produce microstructure with the desired grain shape factor which is not possible in the traditional hexagonal based model microstructure. The random Voronoi sites are varied continuously, using the Monte Carlo simulations, until the desired grain shape factor is obtained. In all the simulations, we have assumed that stress is acting only along the y-directions and multiple crack nucleation sites are present on the left-hand side of the microstructure.

3.2 Model predictions

Besides random texture, the fiber textures assigned in the equiaxed microstructure were of three different types: <100>, <115>, and <023>, assuming ND as the macroscopic fiber axis. The intensities of fiber textures were varied in order to obtain different GBCDs and, in all cases, a stress magnitude (σ) of 651 MPa was applied. For each case, ten Monte Carlo iterations were carried out to account for the various possible orientations and spatial distributions of grain orientations for the same texture descriptions. During each simulation, the maximum crack length and the GBCD were recorded. The predicted crack-length and percolation frequency were taken as the average of the maximum crack length found in each individual simulation and, the percentage of times crack had crossed through the thickness of the sample, respectively.

Fig. 4 shows the comparisons of GBCDs, for 5° and 10° half-widths, in terms of fractions of random and Σ(1-29) boundaries in the microstructure used in the model, as well as the normalized average crack-lengths obtained from the simulations. The detailed GBCDs for 10° half-width fiber textured samples are shown in Fig. 5 to illustrate the specific grain boundary character evolution from a given texture description. For comparison, the detailed GBCD evolved from the random texture input is also shown.

Clearly, unlike the <115> and <023> fiber textured cases, there is a significant fraction of CSL boundaries in the <100> fiber textured samples and, this was not unanticipated since many of the CSL boundaries, such as Σ5, Σ13a, Σ17a, Σ25a, and Σ29a are defined with the <100> misorientation axis and the formation of such boundaries are facilitated by the presence of <100> fiber texture. As also expected, for <100> fiber textured samples, the fractions of LAB and CSL boundaries decrease with the decrease of texture intensity, in other words, with the increase of half-width, and as a result the average crack length increases. The latter is also true for other fiber textured samples although the fraction of CSL boundaries increased with the increased deviation of grain orientations from the ideal fiber descriptions of those samples. However, the increased fractions of CSL boundaries in those samples did not match up with the LABs that decreased more rapidly and, as a

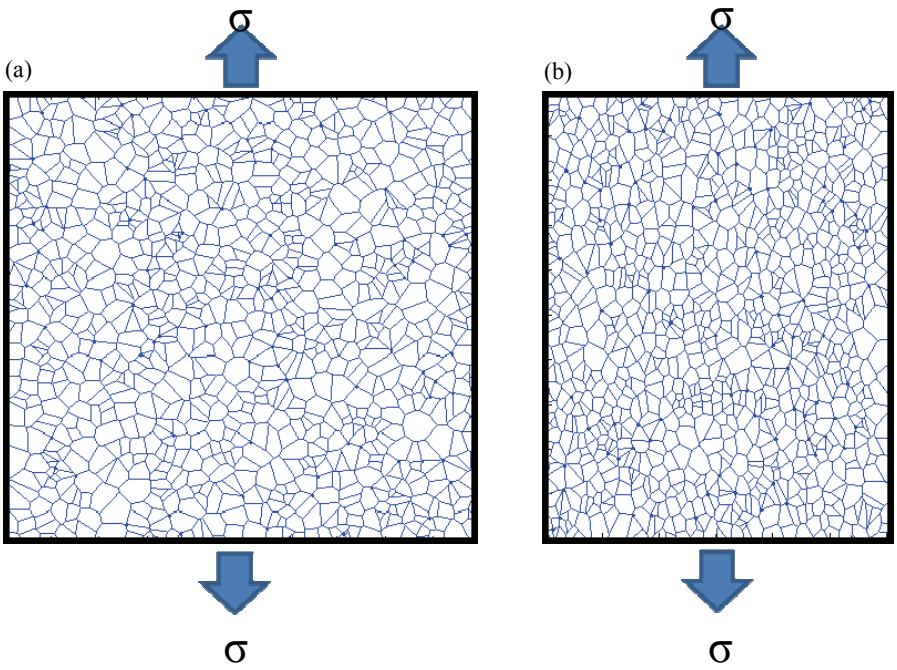

Figure 3: Voronoi microstructures with (a) grain shape factor = 0.52 (near-equiaxed), and (b) grain shape factor = 0.39 (vertically elongated)

result, the number of HABs increased. Also, not all the CSL boundaries within Σ(3-29) have high fracture strengths. An interesting example of having certain Σ boundaries on the overall fraction of Σ(3-29) boundaries could be seen by comparing the crack length of <115> and <023> fiber textured samples and the detailed GBCDs (averaged) shown in Fig. 5. In both samples, for 10° half-width, the overall percentage of CSL boundaries did not vary noticeably (6.23% vs. 6.24%) from each other. However, there are slightly more Σ5 (1.68% vs. 1.7%), Σ13a (1.17% vs. 1.19%), Σ17a (0.44% vs. 0.53%), Σ25a (0.3% vs. 0.33%), and Σ29a (0.27% vs. 0.29%) boundaries generated in case of <023> textured Mo which have high fracture strength values and, therefore, even though the percentage of LAB is lower than that of its counterpart (21.18% vs. 20.9%), the crack-length was little less in this sample (note that, the grain boundary percentage differences mentioned above are the average values based on 10 Monte Carlo iterations). The overall GBCDs should thus be used in caution when predicting the crack-lengths and here lies the advantage of a texture based model which can reproduce the detailed GBCD accurately.

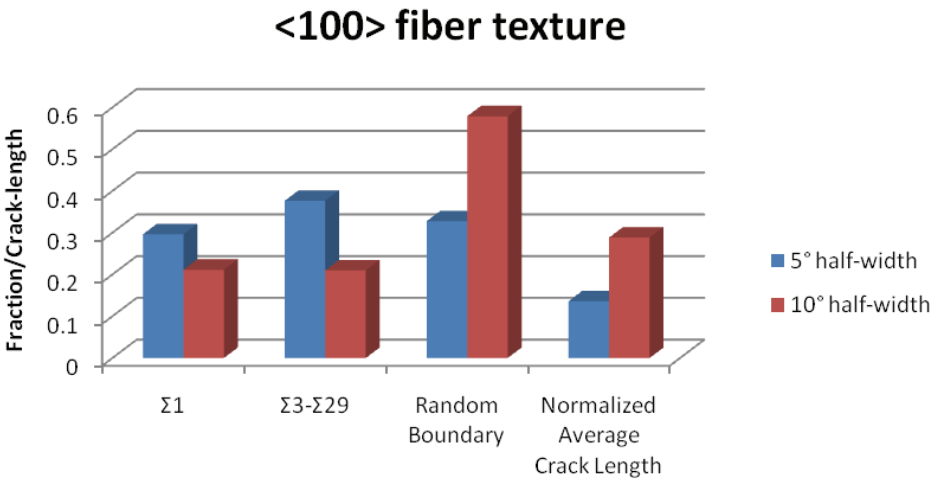
<100> fiber texture
Fraction/Crack-length
0.6
0.5
0.4
0.3
0.2
0.1
0
Σ1
Σ3-Σ29
Random Boundary
Normalized Average Crack Length
5° half-width
10° half-width

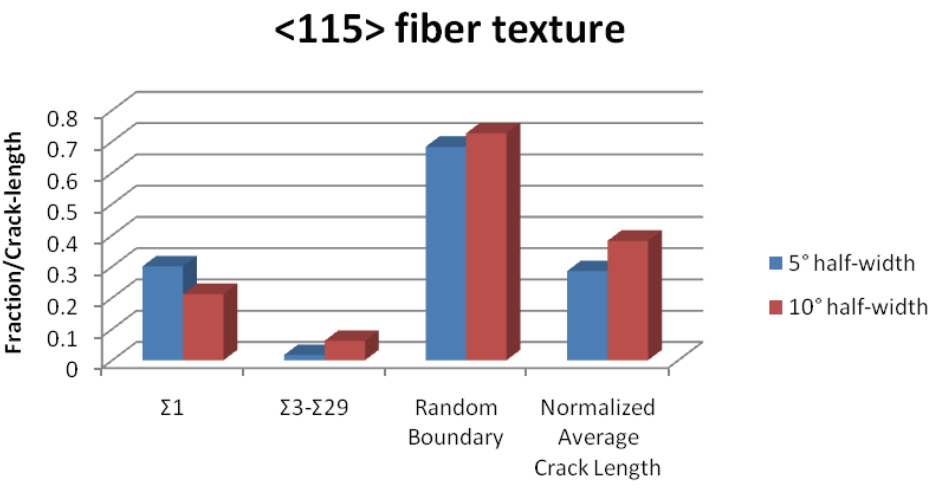
<115> fiber texture
Fraction/Crack-length
0.8
0.7
0.6
0.5
0.4
0.3
0.2
0.1
0
Σ1
Σ3-Σ29
Random Boundary
Normalized Average Crack Length
5° half-width
10° half-width

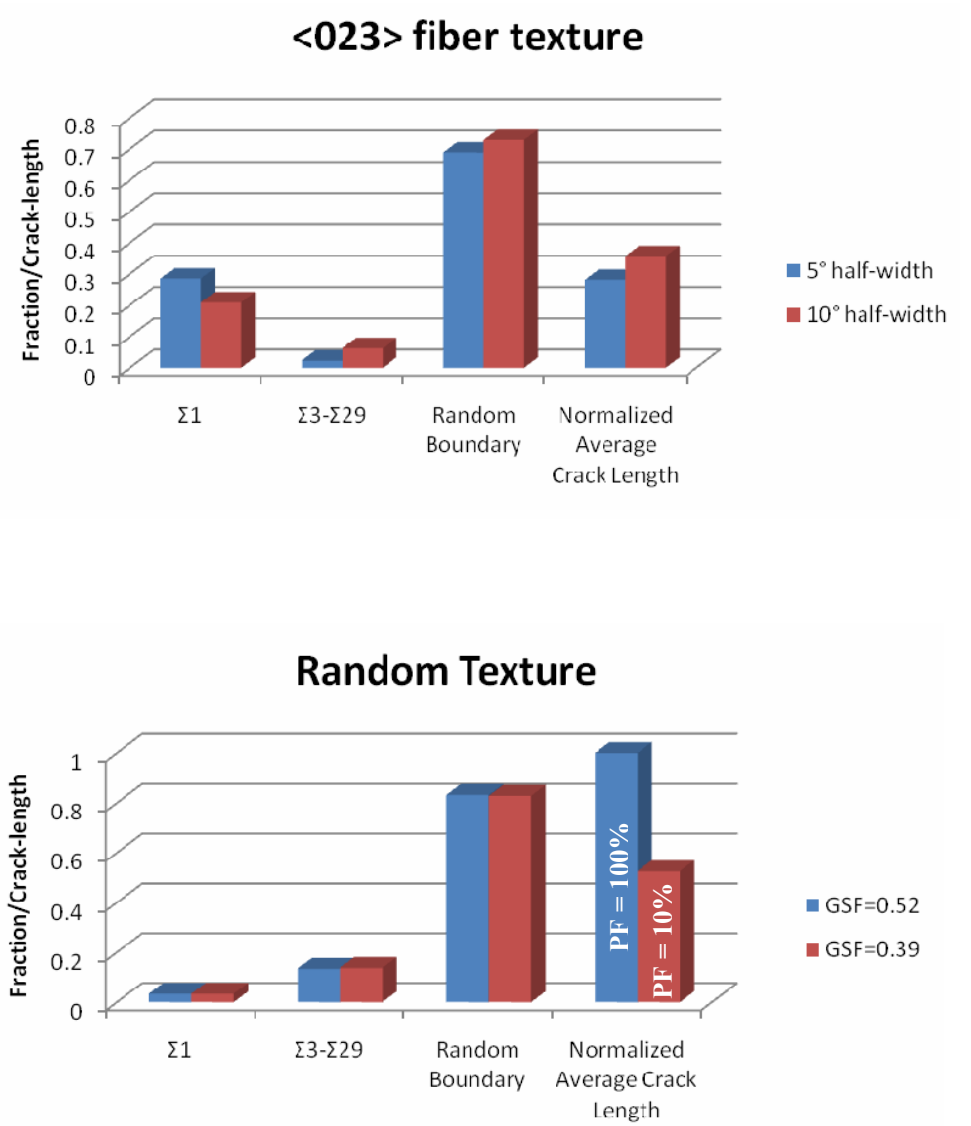

Figure 4: Grain boundary character distributions and the corresponding normalized crack-propagation length for different fiber and random textured samples (PF: percolation frequency)

None of the fiber textured samples showed percolation but, in contrast, in all the random textured samples, percolation was predicted. This, however, was quite predictable because, the overall and detailed GBCDs of random textured sample

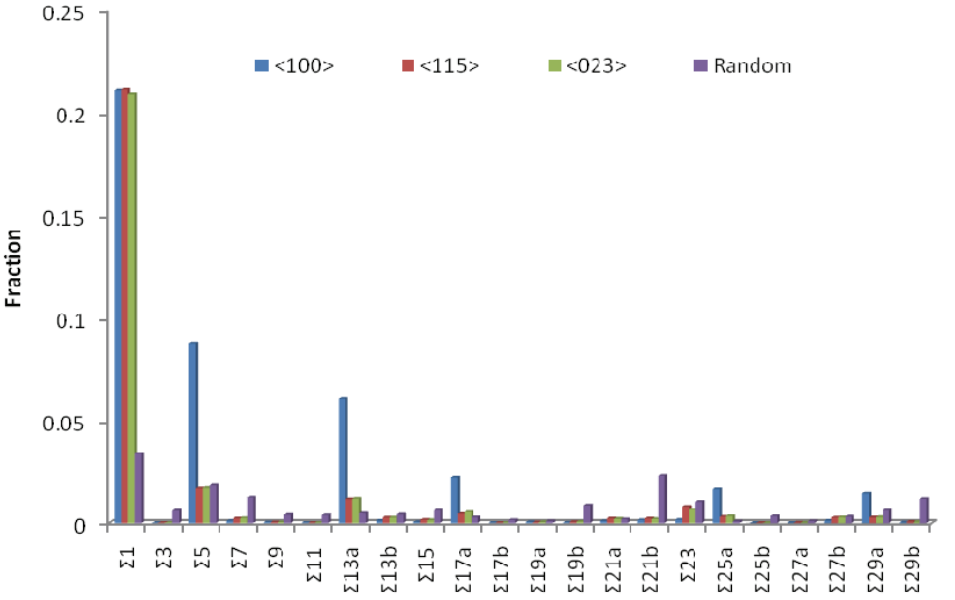

Figure 5: Detailed grain boundary character distribution for different fiber textured samples with 10° half-width and random textured sample

showed very small fraction of crack-resistant boundaries as can be observed in Fig. 5. Thus, it is obvious that the fiber textured samples with higher fraction of low-energy grain boundaries are certainly preferable over the random textured samples. However, random textured samples are of most common type since it is extremely expensive to manufacture the fiber textured samples. One possible remedy to this problem is the manipulation of grain shape because if larger fraction of grain boundaries is unfavorably oriented with respect to the stress direction, crack propagation might be arrested at a safe maximum length. In the current study, we have therefore simulated the crack propagation in a random textured vertically elongated microstructure, shown in Fig. 3b, with a grain shape factor of 0.39. The normalized average crack length and percolation frequency are shown in Fig. 4 which clearly suggests that crack propagation length and percolation frequency could be diminished for low grain shape factor random textured samples.

4 Summary and Conclusions

Intergranular crack propagation in textured polycrystalline materials has been simulated using a novel integrated modeling approach based on Voronoi algorithm, Markov Chain theory, texture and grain boundary character, and Monte Carlo sim-

ulations. The predicted crack propagation behavior is consistent with the well-known understanding of the relationship between the low-energy boundary and their resistance to cracking.

Fiber textured samples are, in general, highly resistant to intergranular damage propagation while the random textured polycrystals are the most vulnerable. However, the fraction of crack-resistant boundaries present in the microstructure depends on the type of fiber texture and decreases significantly with the increase of half-width or, in other words, with the decrease of texture intensity.

It has been shown that the overall GBCD, often used as input to assess the crack-propagation extent could be sometimes misleading and texture based model could help overcome this limitation.

Study of the model microstructures with different grain shape factors suggests that the crack propagation behavior can be effectively controlled in highly susceptible random polycrystals by suitably manipulating the grain shapes when obtaining the increased fraction of low-energy crack resistant boundaries is not feasible.

Acknowledgement: The authors would like to acknowledge financial supports from the Natural Science and Engineering Research Council (NSERC) of Canada and McGill University.

References

Arafin, M. A.; Szpunar, J. A. (2009a): A new understanding of intergranular stress corrosion cracking resistance of pipeline steel through grain boundary character and crystallographic texture studies. *Corros. Sci.,* vol. 51, no. 1, pp. 119-128.

Arafin, M. A.; Szpunar, J. A. (2009b): A Markov Chain - Monte Carlo model for intergranular stress corrosion crack propagation in polycrystalline materials. *Mater. Sci. Eng. A,* vol. 513-514, pp. 254-266.

Arafin, M. A.; Szpunar, J. A. (2009c): Modeling the effect of grain clustering on the intergranular crack propagation behavior in polycrystalline materials. *Comput. Mater. Sci.,* vol. 46, no. 4, pp. 932-941.

Arafin, M. A.; Szpunar, J. A. (2009d): A novel microstructure-grain boundary character based integrated modeling approach of intergranular crack propagation in polycrystalline materials. *Comput. Mater. Sci.,* vol. 47, pp. 890-900.

Brosse, J. B.; Fillit, R.; Biscondi, M. (1981): Intrinsic intergranular brittleness of molybdenum. *Scripta Metall.,* vol. 15, no. 6, pp. 619-623.

Crawford, D. C.; Was, G. S. (1992): The role of grain boundary misorientations in intergranular cracking of Ni-16Cr-9Fe in 360˚C argon and high purity water,

Metall. Mater. Trans. A, vol. 23, pp. 1195-1206.

Gertsman, V. Y.; Tangri, K. T. (1997): Modeling of intergranular damage propagation, *Acta Materialia,* vol. 45, no. 10, pp. 4107-4116.

Gertsman, V. Y.; Bruemmer, S. M. (2001): Study of grain boundary character along intergranular stress corrosion crack paths in austenitic alloys, *Acta Mater.,* vol. 49, no. 9, pp. 1589-1598.

Ikeda, K.; Morita, K.; Nakashima, H.; Abe, H. (1999): Misorientation dependence of grain boundary fracture strength and grain boundary energy for molybdenum <001> symmetric tilt boundaries. *J. Japan Inst. Metals,* vol. 63, no. 2, pp. 179-186.

Jivkov, A.P.; Stevens, N.P.C.; Marrow, T.J. (2006): A two-dimensional model for intergranular stress corrosion resistance, *Acta Mater.,* vol. 54, no. 13, pp. 3493-3501.

Kurishita, H.; Oishi, A.; Kubo, H.; Yoshinaga, H. (1983): Grain boundary fracture in molybdenum bicrystals with a <110> direction symmetric tilt boundary. *J. Japan Inst. Metals,* vol. 47, no. 7, pp. 546-554.

Lim, L. C.; Watanabe, T. (1990): Fracture toughness and brittle-ductile transition controlled by grain boundary character distribution (GBCD) in polycrystals. *Acta Metall. Mater.,* vol. 38, no. 12, pp. 2507-2516.

Lin, H.; Pope, D. P. (1993): The influence of grain boundary geometry on intergranular crack propagation in Ni3Al, *Acta Metall. Mater.,* vol. 41, no. 2, pp. 553-562.

Lin, H.; Pope, D. P. (1995): Weak boundaries in Ni3Al, *Mater. Sci. Eng. A,* vol. 192-193, pp. 394-398.

Mykura, H. (1980): *A checklist of cubic coincidence site lattice relations, in: Grain Boundary Structure and Kinetics*, ASM Materials Science Seminar, ASM International.

Palumbo, G.; King, P. J.; Aust, K. T.; Erb, U.; Lichtenberger, P. C. (1991): Grain boundary design and control for intergranular stress corrosion resistance, *Scripta Metall.,* vol. 25, no. 8, pp. 1775-1780.

Pan, Y.; Olson, T.; Adams, B. L. (1995): Applications of orientation imaging analysis to microstructural control of intergranular stress corrosion cracking, *Can. Metall. Q.,* vol. 34, no. 3, pp. 147-154.

Pan, Y.; Adams, B. L.; Olson, T.; Panayotou, N. (1996): Grain-boundary structure effects on intergranular stress corrosion cracking of alloy X-750, *Acta Mater.,* vol. 44, no. 12, pp. 4685-4695.

Shi, J.; Zikri, M. A. (2009): Grain-boundary interactions and orientation effect

on crack behavior in polycrystalline aggregates. *Int. J. Solids Struct.*, Vol. 46, pp. 3914-3925.

Tanaka, T.; Tsurekawa, S.; Nakashima, H.; Yoshinaga, H. (1994): Misorientation dependence of fracture stress and grain boundary energy in molybdenum with <110> symmetric tilt-boundaries. *J. Japan Inst. Metals,* vol. 58, no. 4, pp. 382-389.

Tsurekawa, S.; Kokubun, S.; Watanabe, T. (1999): Effect of grain boundary microstructures of brittle fracture in polycrystalline molybdenum. *Mater. Sci. Forum,* vol. 304-306, pp. 687-692.

Tsurekawa, S.; Tanaka, T.; Yoshinaga, H. (1994): Grain boundary structure, energy and strength in molybdenum. *Mater. Sci. Eng. A.,* vol. 176, pp. 341-348.

Wang, G.; Zuo, L.; Esling, C. (2002): Computer simulation on the tendency of intergranular fracture in textured polycrystalline materials. *Philos. Mag. A.,* vol. 82, no. 12, pp. 2499-2510.

Watanabe, T. (1984): An approach to grain boundary design for strong and ductile materials, *Res. Mechanica,* vol. 11, pp. 47-84.

Watanabe, T.; Tsurekawa, S. (1999): The control of brittleness and development of desirable mechanical properties in polycrystalline systems by grain boundary engineering. *Acta Mater.,* vol. 47, no. 15, pp. 4171-4185.

Watanabe, T. (1994): The impact of grain boundary character distribution on fracture in polycrystals. *Mater. Sci. Eng. A.,* vol. 176, pp. 39-49.

Wells, D. B.; Stewart, J.; Herbert, A. W.; Scott, P. M.; Williams, D. E. (1989): The use of percolation theory to predict the probability of failure of sensitized, austenitic stainless steels by intergranular stress corrosion cracking. *Corros.,* vol. 45, no. 8, pp. 649-660.